

WFC3 TV3 Testing: Quantum Yield of the UVIS CCDs

T. Borders, P. McCullough, S. Baggett
July 13, 2010

ABSTRACT

We measure the quantum yield (technically, the true quantum yield plus the Fano factor) from a large set of monochromatic narrowband post-TV3 flatfields taken with WFC3 in the UVIS channel. Our analysis results show that the quantum yield is ~30% less than predicted, in good agreement with earlier results based on a small set of broadband UV filters (Baggett 2008).

Introduction

The quantum yield is the number of charge carriers generated per interacting photon (Janesick 2001). For CCD detectors in the optical, each detected photon usually generates a single electron resulting in a quantum yield equal to 1. However, with higher energy UV photons, there is a non-zero probability of creating more than one electron per detected photon resulting in quantum yield >1 .

The theoretical quantum yield is the energy of the incoming photon $E(\text{eV}) = hc/\lambda$ divided by the energy needed to produce an e- hole pair in silicon (3.65 eV/e-, at room temperature) (Janesick 2001) or quantum yield of 1.7 e-/photon at 200nm decreasing to 1.0 at 340nm. Data from WFC3 Thermal-Vacuum test #3 (TV3) showed indications that the quantum yield was not as large as expected: measurements in F218W, F225W, F275W and F336W were 30% less than the predictions (Baggett 2008), possibly due to charge sharing (Janesick 2007).

The goal of our analysis is to add additional measurements of the quantum yield. The analysis reported here makes use of the post-TV3 monochromatic flats taken in the SSDIF (Space Systems Development and Integration Facility) at wavelengths 208nm, 224nm, 240nm, 256nm, 272nm, 288nm, 304nm, 320nm, 336nm, 352nm, and 368nm.

Observations and Analysis

The flatfields used in this quantum yield analysis are summarized in Table 1. The flat field images were produced using narrow-band monochromator settings of the external WFC3 stimulus (CASTLE). Wavelength settings ranged from 208 to 400nm at steps of 16nm. The CASTLE deuterium (D2) lamp was used at the 3 shortest wavelengths and the Xenon (Xe) lamp was used for the remainder. The same exposure time was used for pairs of images taken at each wavelength. All the data were acquired over two to three days with WFC3 in an ambient environment and the UVIS detector at a temperature of -49C.

Calwf3 version 1.1 was used to process all images in order to remove the bias overscan level (blevcorr=perform and dqicorr=perform) and average and difference images were created from pairs of bias-subtracted images. Baggett (2008) used the mean-variance methodology to compute the nominal instrument gain by plotting the mean signal level versus the variance, so that the reciprocal of the slope is the gain (referred to as J in equation 2.9 in Janesick (2001)). The mean levels were measured on the average images and the variance were taken from the difference images (standard deviation squared divided by 2). The statistics were computed using 3 iterations of 3 sigma clipping.

Each flat was taken as a full-frame image so for consistency with the prior study, we performed our image statistics on the same subarray (1024x1024) region positioned in the outer corner of the C amplifier on CCD Chip #2 (science image FITS file extension [1]) and excluded columns 1-200 and rows 1-200 in the statistics in order to avoid the vignetting in the CASTLE illumination pattern. We also performed our analysis on the same subarray region positioned on the outer corner of the A amplifier on CCD Chip #1 (science image FITS file extension [4]). However, for our data, exposure times for a given wavelength were identical, so we could not use the mean-variance methodology. The broadband data in the previous study were taken at multiple signal levels at each wavelengths, enabling a standard photon transfer curve analysis, whereas we had only a single signal level at each wavelength and had to devise a slightly different method of analysis. We use the overscan of each image to determine the variance corresponding to a mean signal of zero photons, and from the same image's previously-described 1024x1024 subarray, we measure the variance and mean of the CCD's response to illumination at each specific wavelength. Those two points in the variance-vs-mean plot define a line, the inverse slope of which we tabulate in Table 2 (gain) for each measured wavelength of the illumination.

The quantum yield parameter in this report is calculated as the ratio of the gain in the visible to the gain in the UV (Janesick 2001). While this is technically a "gain ratio" we will continue to henceforth refer to it as the quantum yield. Note, however, that what we are calling the "quantum yield" is in fact the sum of the true quantum yield η and the Fano factor F (McCullough et al. 2008, Equation 30). Our gain data show an offset of $\sim 4.6\%$ from the gain measurements of Baggett (2008); however, normalizing our data so that our longest wavelength measurement has a quantum yield of 1 places

our observations in agreement. There are at least four subtle effects which may account for the gain differences. (1) As described earlier, the previous analysis made use of the standard mean-variance methodology, whereas this was not possible with our data due to data limitations. (2) The CCD detector could be slightly non-linear in its response, which we have neglected (as in the previous study before us though they limited their measurements to data well within better than 1% nonlinearity). Nevertheless, because our exposure levels tend to be much lower than those of the previous study, we would expect any uncorrected non-linearity to affect our results differently. (3) The CCD detector's spatial non-uniformity will slightly affect the photon transfer curve, although its effect is mitigated by selecting a relatively uniform subarray and by maintaining a stable lamp brightness for each exposure. (4) The operating temperature of the CCD was -82C in the data from the previous study, which is the normal flight operating temperature, while our data were acquired at a CCD temperature of -49C. While these four effects may have perturbed the measured gain, we do not expect them to affect significantly the quantum yield.¹ Consequently, we divided each of our measured gains by the gain that we measured at 400nm, the wavelength at which we expect the quantum yield to equal unity.

Figure 1 shows our quantum yields plotted as a function of wavelength for CCD Chip #1 (blue), CCD Chip #2 (purple) and the quantum yield measurements from Baggett (2008) (red). Si I measurements from Wilkinson (1983) are also shown in Figure 1 (green). Figure 2 also shows the measured quantum yields as a function of energy.

Figure 3 presents the relative quantum yield on a log scale as a function of wavelength. The WFC3 UVIS detector's QY excess is approximately 1/3 that of Wilkinson et al. at wavelengths in common. Also plotted in Figure 3 are the original Wilkinson (1983) data and the Wilkinson data scaled by 1/3. The latter provides a reasonable match to the results for CCD Chip #2 and to a lesser degree, CCD Chip #1, which for unknown reasons, shows a significant dip at ~ 320 nm. A simple quadratic form for the quantum yield $\hat{\eta}$ that matches the WFC3 data is²

$$\hat{\eta} = 1 + A (h\nu - E_0)^2, \quad (1)$$

where the relation is valid in the range $E_{max} > h\nu > E_0$, where our measurements extend to $E_{max} = 6$ eV, the threshold for greater-than-unit quantum yield is $E_0 = 3.2$ eV, and empirically, $A \sim 0.015$ eV⁻².

Figure 4 shows the relative quantum yields as a function of 1/wavelength along with the best quadratic fit to the data scaled by 1/3. Figure 5 shows quantum yield as a function of energy. A quadratic function is fit to these data as well as Wilkinson (1983) scaled by 1/3.

¹Theoretically, the temperature dependence of the quantum yield of silicon is less than 4% from 0 K to 300 K (Figure 1 of Groom 2004; Sirianni & Pavlovsky 2006)

²The ratio of gains, $\hat{\eta} = F + \eta$, where F is the Fano factor and η is the quantum yield (see Equation 30 of McCullough et al. 2008 for details). For simplicity in this report we refer to $\hat{\eta}$ as the quantum yield, with the understanding that $\hat{\eta}$ includes the Fano factor implicitly.

Table 1. List of flatfields. All images were full-frame UVIS.

Tvnum Range	Monochromator Wavelength (nm)	Observation Dates	Exposure Time (sec) per image	Lamp
59452-59592	208	2008-07-19 to 2008-07-21	500	D2
59449-59589	224	2008-07-19 to 2008-07-21	1200	D2
59447-59586	240	2008-07-19 to 2008-07-21	1250	D2
59435-59576	256	2008-07-19 to 2008-07-20	700	Xe
59433-59572	272	2008-07-19 to 2008-07-20	750	Xe
59431-59570	288	2008-07-19 to 2008-07-20	383	Xe
59441-59580	304	2008-07-19 to 2008-07-20	240	Xe
59440-59579	320	2008-07-19 to 2008-07-20	140	Xe
59439-59578	336	2008-07-19 to 2008-07-20	90	Xe
59438-59577	352	2008-07-19 to 2008-07-20	70	Xe
59436-59575	368	2008-07-19 to 2008-07-20	60	Xe
59434-59573	384	2008-07-19 to 2008-07-20	50	Xe
59432-59571	400	2008-07-19 to 2008-07-20	40	Xe

Table 2. Gain and quantum yield as a function of wavelength. Quantum yields are in units of e-/interacting photon.

Wavelength (nm)	Energy (eV)	Gain Chip #1, #2	Quantum Yield Chip #1, #2
208	5.961	1.474, 1.512	1.093, 1.093
224	5.535	1.492, 1.506	1.080, 1.097
240	5.166	1.513, 1.541	1.065, 1.072
256	4.843	1.550, 1.582	1.040, 1.045
272	4.558	1.543, 1.610	1.044, 1.026
288	4.305	1.569, 1.597	1.027, 1.035
304	4.078	1.593, 1.627	1.012, 1.016
320	3.874	1.628, 1.641	0.989, 1.007
336	3.690	1.612, 1.645	0.999, 1.005
352	3.522	1.594, 1.638	1.011, 1.009
368	3.369	1.613, 1.649	0.999, 1.003
384	3.229	1.614, 1.653	0.998, 1.000
400	3.100	1.611, 1.653	1.000, 1.000

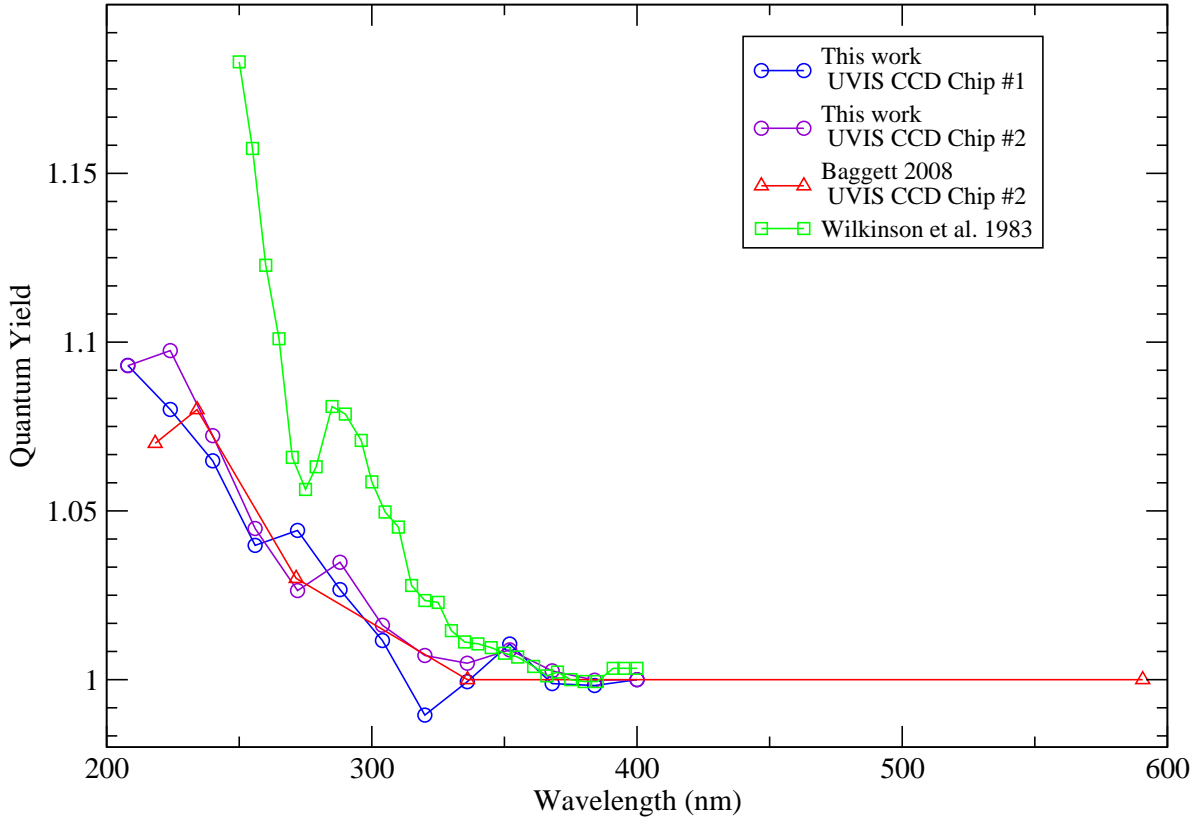


Figure 1. Our resulting quantum yields are plotted as a function of wavelength (blue and purple); the Baggett 2008 measurements are plotted in red and the quantum yield measurements of Si I by Wilkinson 1983 results are shown in green.

Conclusions

The quantum yields have been measured in a set of ground based narrowband flat fields in the UV. Our quantum yield results compare favorably, after a normalization, to previous WFC3 results (Baggett 2008) as well as to Si I measurements (Wilkinson et al., 1983). Several subtle effects, such as CCD temperature differences between the datasets, or small non-linearity and/or spatial non-uniformities in the chips, may account for the differences between our gains and those in Baggett (2008). However, normalizing our data so that the longest wavelength measurement has a quantum yield of 1 places our narrowband observations in good agreement with the prior broadband results.

Acknowledgments

Thanks to all members of the extended WFC3 team who supported the thermal vacuum tests.

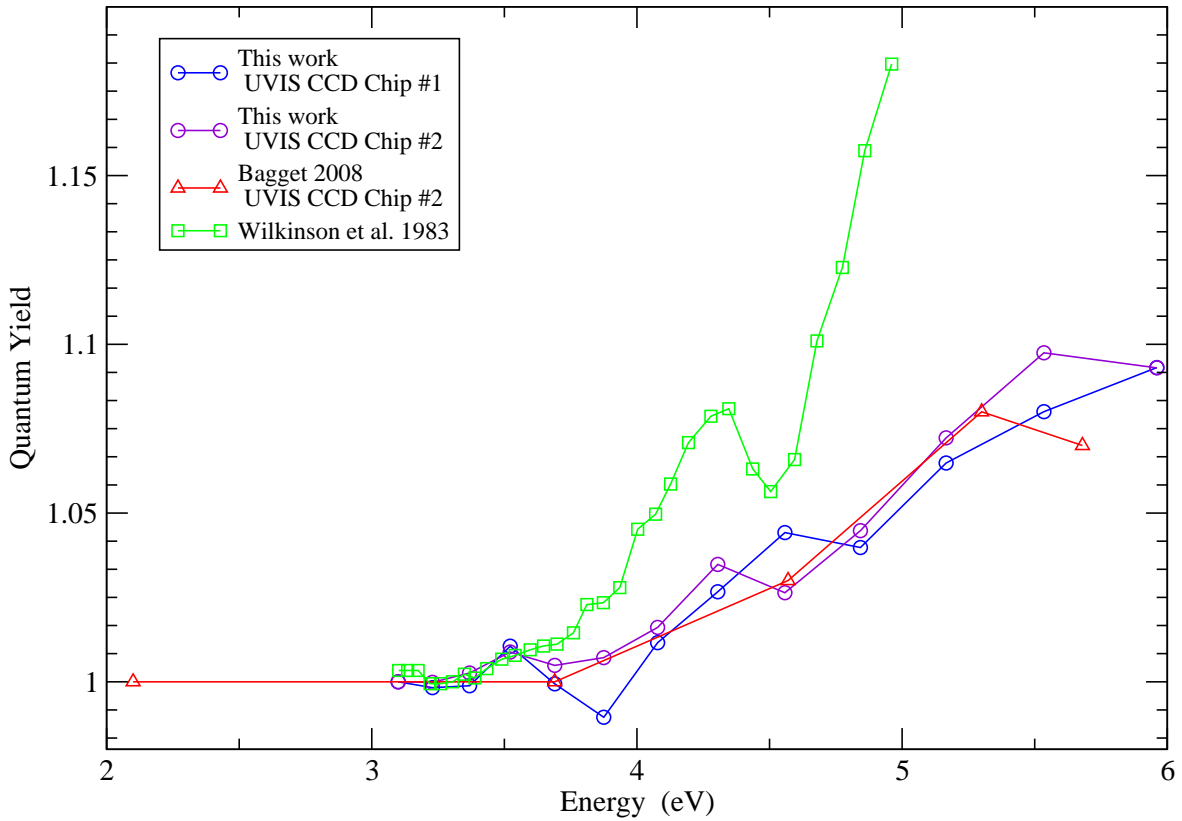


Figure 2. Our resulting quantum yields are plotted as a function of energy (blue and purple); the Baggett 2008 measurements are plotted in red and the quantum yield measurements of Si I by Wilkinson 1983 are shown in green.

References

- Baggett, S., 2008, WFC3 ISR 2008-47, "WFC3 TV3 Testing: Quantum Yield in the UV."
- Baggett, S., 2008, WFC3 ISR 2008-13, "WFC3 TV3 Testing: UVIS-1' Gain Results."
- Janesick, J., 2001, "Scientific Charge-Coupled Devices," Chapters 2 & 3, SPIE Press, Bellingham, WA.
- McCullough, P.R., Regan, L., Bergeron, L., & Lindsay, K., 2008, PASP, 120, 759
- Wilkinson, F.J., Farmer, A.J.D., & Geist, J. 1983, J. Appl. Phys., 54,1172

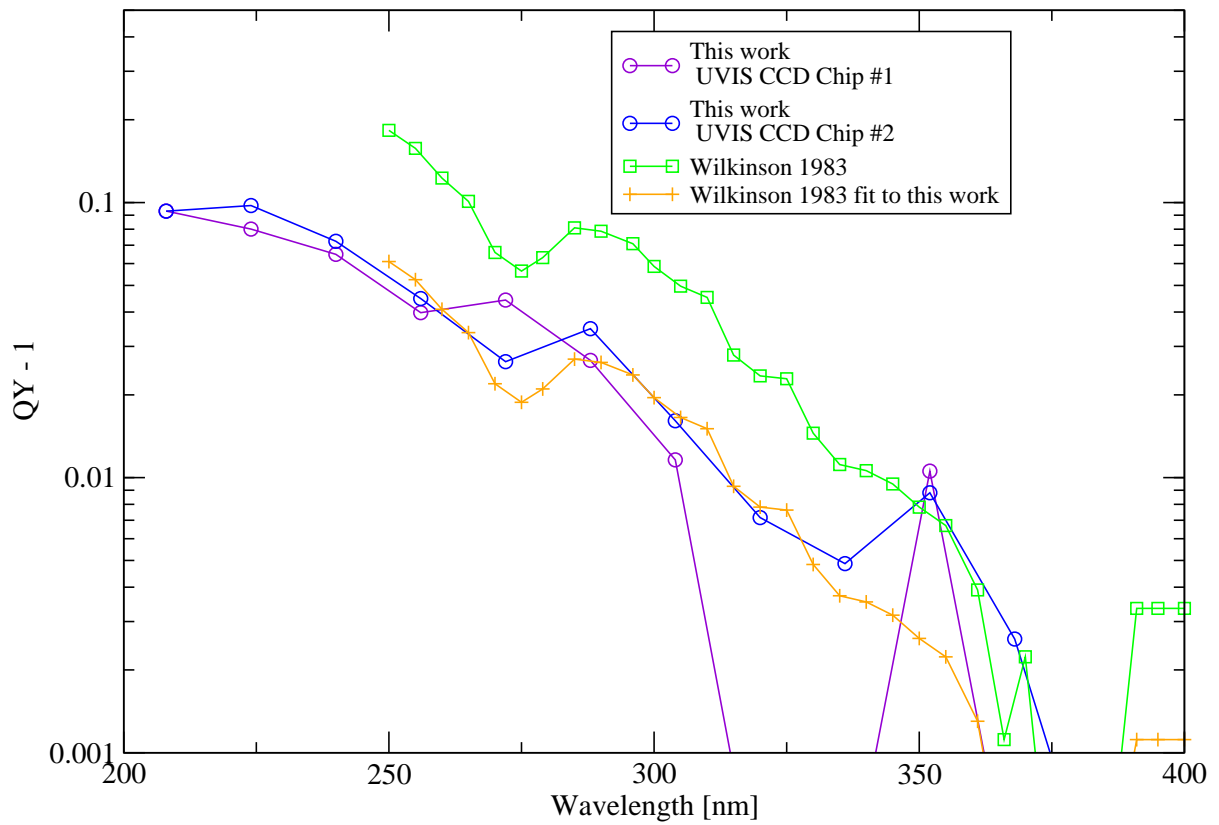


Figure 3. This figure shows quantum yields -1 on a log scale as a function of wavelength for this work (blue and purple), the original Wilkinson 1983 data (green) and the Wilkinson data scaled by 1/3 (orange).

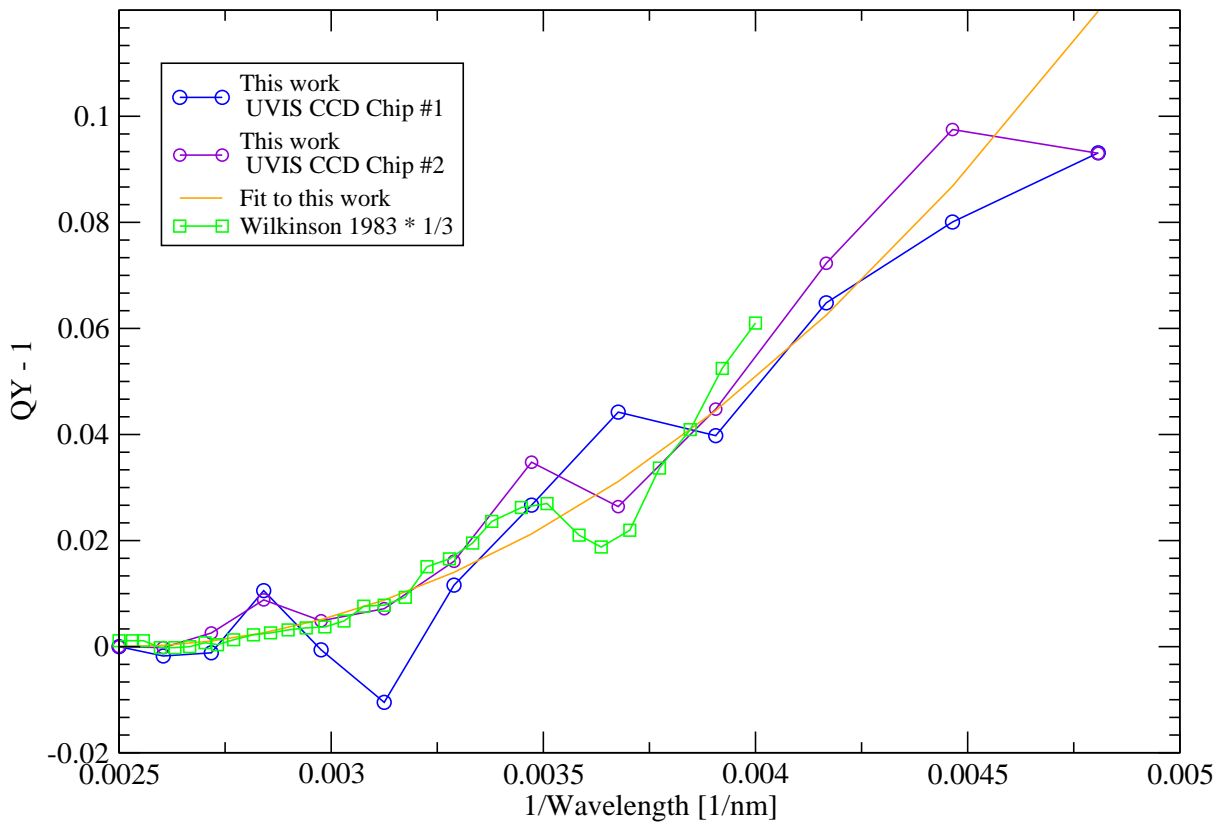


Figure 4. This figure shows quantum yields -1 as a function of 1/wavelength (blue and purple) overplotted is a quadratic fit (equation 1) to these data (Equation 1 in orange) as well as the Wilkinson 1983 data (green) scaled by 1/3.

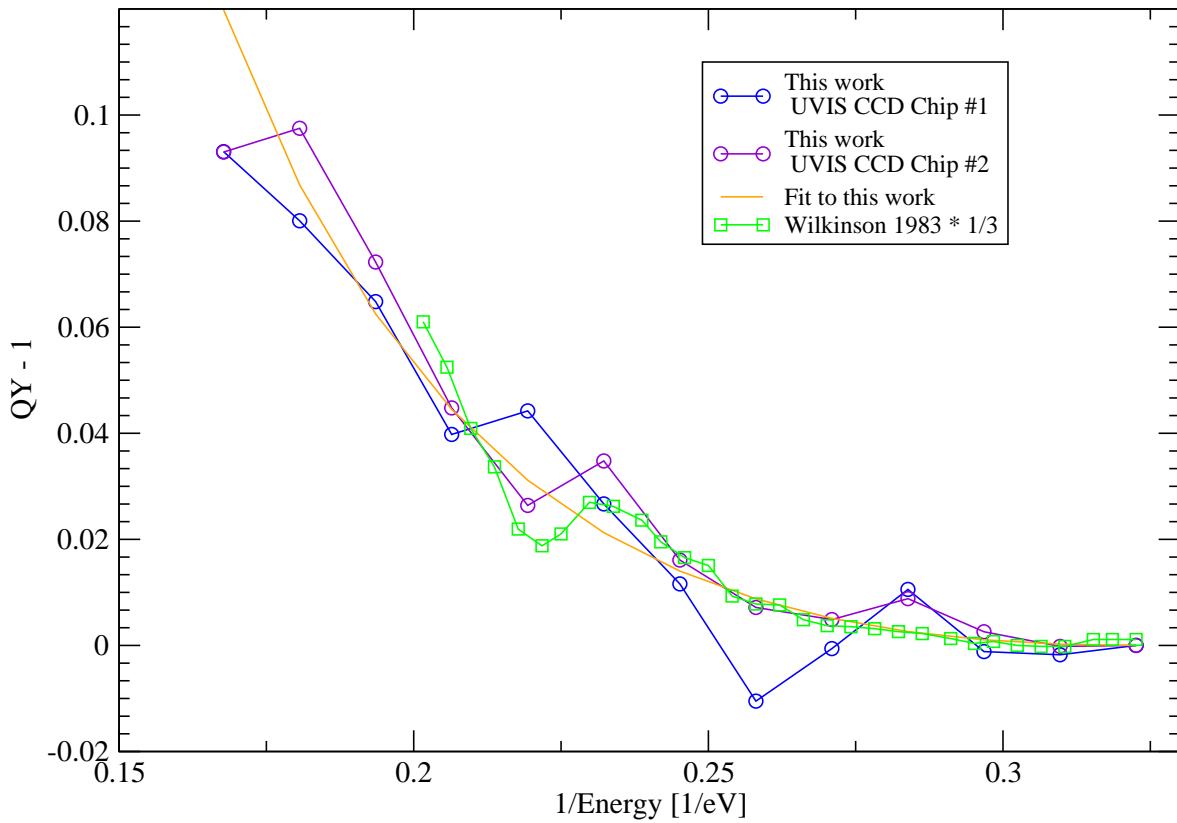


Figure 5. Figure shows quantum yields -1 for this work as a function of 1/energy (blue and purple), a quadratic fit to these data (orange) as well as Wilkinson 1983 data scaled by 1/3 (green).